Atmospheric forcing of the Beaufort Sea ice gyre: Surface-stratosphere coupling

J. V. Lukovich,[1] M. G. Asplin,[1] and D. G. Barber[1]

Received 1 April 2008; revised 24 July 2008; accepted 27 August 2008; published 17 January 2009.

[1] In a companion article we examined the nature of correspondence between synoptic weather patterns and reversals in the Beaufort Sea ice gyre. In this paper we extend this analysis to examine the role of stratospheric forcing on surface phenomena. Investigated in particular is the correspondence between reversals in stratospheric winds at 10 mbar during winter as defined by stratospheric sudden warmings (SSW) and mean sea level pressure synoptic types in the Beaufort Sea region. Connections between stratospheric and surface events are characterized using relative vorticity and the square of strain computed at different pressure levels from the stratosphere to the surface in the Beaufort Sea region. We quantify the correspondence between stratospheric flow and surface phenomena through investigation of the frequency in synoptic types derived in a companion article during stratospheric sudden warming events. Investigation of stratospheric wind gradients averaged over the Beaufort Sea region demonstrates a prevalence in anticyclonic activity during SSWs that persists for approximately 20 days. Examination of the evolution in synoptic types in the Beaufort Sea region also shows an increase in the number of synoptic types associated with anticyclonic activity during SSWs.

Citation: Lukovich, J. V., M. G. Asplin, and D. G. Barber (2009), Atmospheric forcing of the Beaufort Sea ice gyre: Surface-stratosphere coupling, *J. Geophys. Res.*, *114*, C00A03, doi:10.1029/2008JC004849.

1. Introduction

[2] A companion article (M. Asplin et al., Atmospheric forcing of the Beaufort Sea Ice Gyre: An examination of synoptic weather patterns preceding summer circulation reversal events, submitted to *Journal of Geophysical Research*, 2008) created a catalogue of synoptic types for the Beaufort Sea region (BSR) using NCEP-NCAR gridded mean sea level pressure (SLP), and a two-step principal components analysis and k-means typing algorithm, and then examined synoptic weather patterns preceding summer reversals in the Beaufort Gyre (BG). In this study we examine the connection between stratospheric variability as depicted by stratospheric sudden warmings (SSWs), and surface cyclone types in the Beaufort Sea region (BSR). The evolution in wind gradient fields during SSWs is also investigated for comparison of atmospheric circulation from the stratosphere to the surface at hemispheric and regional scales.

[3] Stratospheric sudden warmings, which are associated with disturbances to the polar vortex due to upward propagating planetary waves (PWs) during winter, govern Arctic wintertime variability in the stratosphere. Defined as the transition from westerly to easterly zonal mean winds at 60°N and 10 mbar, SSWs are characterized by a rapid increase in stratospheric temperatures over several days and a deceleration in the zonal jet, with implications for the cyclonic circulation that characterizes the polar vortex, exchange between polar and midlatitude air, and stratosphere-troposphere exchange [*Shepherd*, 2002; *Scott and Polvani*, 2006; *Charlton and Polvani*, 2007a, 2007b]. Previous studies have documented an unprecedented increase in SSWs over the last decade, with a paucity of SSWs during the 1990s [*Manney et al.*, 2005; *Charlton and Polvani*, 2007a]. An SSW of unprecedented duration was detected during the 2003–2004 winter, with a vortex disruption occurring for two months [*Manney et al.*, 2005]. Typical disruptions are on the order of days to weeks.

[4] The role of SSWs in illustrating coupling between the troposphere and stratosphere is reflected in studies that have highlighted the correspondence between stratospheric events such as SSWs and extreme stratospheric events (ESEs, defined as days during which the Northern Annular Mode (NAM) index exceeds the absolute value of a given threshold) as a consequence of upward wave activity near the tropopause [*Polvani and Waugh*, 2004; *Charlton and Polvani*, 2007a]. *Polvani and Waugh* [2004] indicated that wave activity originates in the troposphere; large wave activity precedes weak vortex events because of the deposition of westerly momentum in the stratosphere with wave breaking as the upward propagating waves disturb the polar vortex. Strong vortex events are preceded by weak wave activity. Similar connections were found in a study of ozone transport in the polar stratosphere: weaker PW activity allows the cold polar vortex to remain intact as a "containment vessel" for ozone destruction, whereas an increase in PW activity erodes the edge of the polar vortex, resulting in the formation of filaments at the edge, and allowing for the

[1]Centre for Earth Observation Science, University of Manitoba, Winnipeg, Manitoba, Canada.

0148-0227/09/2008JC004849$09.00

exchange between polar and midlatitude air [*Strahan*, 2002]. Studies have also shown that stratospheric anomalies are reflected at the surface for up to 60 days [*Baldwin and Dunkerton*, 2001; *Thompson et al.*, 2002; *Baldwin et al.*, 2003], while *Polvani and Waugh* [2004] demonstrated that surface phenomena are an artifact of wave propagation in the troposphere. In addition, stratospheric anomalies have been shown to propagate to the surface on timescales of two to three weeks, whereas stratospheric NAM anomalies demonstrated maximum predictability of sea level pressure (SLP) over two months during winter [*Baldwin et al.*, 2003].

[5] In recognition of the need for models to accurately capture SSWs in order to improve our understanding of stratosphere-troposphere coupling and exchange mechanisms between the stratosphere and surface, *Charlton and Polvani* [2007a] (hereinafter referred to as CP07) constructed modeling benchmarks and a climatology for SSWs from 1959–2003. SSWs were further categorized into vortex splitting events, whereby the polar vortex is separated into two vortices, and vortex displacement events, whereby the polar vortex is displaced off the pole generating what is referred to as a ''comma shape'' feature associated with the formation of filaments at the edge of the polar vortex.

[6] The climatological study of SSWs by CP07 showed that strong tropospheric zonal flow is required for the formation of a vortex split, and that the structure of the stratosphere and troposphere differ prior to a SSW event. Here it was also shown that strong positive geopotential height anomalies over the Pacific sector accompany vortex split events (CP07, Figure 10b), while tropospheric responses to SSW split and displacement events were similar. Given the stochastic nature of the NAM index it is reasonable to assume that it does not provide a complete description of stratosphere-surface coupling. This has been confirmed in recent studies highlighting a continued decline in sea ice extent despite a neutral NAM state following 1995, suggesting that other scale of processes are required to explain Arctic climate change [*Overland and Wang*, 2005; *Comiso*, 2006]. Recent studies [*Maslanik et al.*, 2007] attribute three regional atmospheric circulation patterns, whose in-phase relationship with the NAM prior to 1995 was replaced by dominant contributions from two circulation patterns following 2000, to a continued decline in sea ice cover in the western Arctic. In addition, vortex split events were shown to occur predominantly in January and February, while vortex displacements occurred throughout winter. It is this climatology that is used in the present investigation to examine the evolution in wind gradients from the stratosphere to the surface, and to provide a link to the climatology of synoptic types documented by Asplin et al. (submitted manuscript, 2008).

[7] In an investigation of the relationship between anticyclones and stratospheric polar vortices, *Harvey et al.* [2002] demonstrated that the merging of stratospheric polar anticyclones gives rise to vortex splitting. Here it was also shown that a deep region or ''well'' of anticyclones exists from the surface to the upper atmosphere from 65°N–85°N during fall and winter, because of the displacement of the polar vortex toward the date line, which coincides with the Aleutian High at 10 mbar. It was further shown that anticyclones accompany polar vortex displacement and continue to exist following SSWs. In addition, Canadian SSWs are associated with a strengthening of the Aleutian High that is characteristic of anticyclonic activity, and its eastward advection to 90°W in a matter of days. Moreover, competition between the anticyclonic Aleutian High and polar vortex results in polar vortex displacement from the pole.

[8] Studies exploring the atmospheric forcing of sea ice have demonstrated connections between summer ice conditions and the winter NAM phase [*Deser et al.*, 2000; *Drobot and Maslanik*, 2003]. Recent studies have examined the relationship between sea ice concentration anomalies and changes in tropospheric zonal mean flow [*Sokolova et al.*, 2007]. Here it was shown that high sea ice cover phases in the Arctic give rise to an increase in wave flux in the middle troposphere from 30°N–70°N associated with baroclinic waves at synoptic timescales ranging from 2 to 6 days. A compensating decrease in wave flux is observed poleward of 60°N because of PWs at seasonal timescales (~10–90 days), resulting in a reduction in the zonal tropospheric flow.

[9] The purpose of the present investigation is to establish a connection between stratospheric and surface phenomena, as an extension to the analysis of the correspondence between cyclonic weather type events in the BSR and BG circulation presented by Asplin et al. (submitted manuscript, 2008). SSWs provide one tool with which stratospheric events may be linked to daily synoptic types in the BSR, and are employed in the present analysis following the climatological assessment of *Charlton and Polvani* [2007a]. Investigation of the evolution in wind gradients during SSWs further enables a comparison of atmospheric circulation from the stratosphere to the surface at hemispheric and regional scales, while providing an alternative to the NAM description as a measure of connections between stratospheric and surface phenomena. In an attempt to understand the correspondence between upper atmospheric dynamics and synoptic activity in the BSR, we therefore examine the following three research questions:

[10] 1. What is the nature of correspondence between wind gradients and SSWs? (SSWs and stratospheric wind gradients.)

[11] 2. What is the nature of wind gradient evolution during SSWs from the stratosphere to the surface? (Stratosphere-surface evolution in wind gradients during SSWs.)

[12] 3. What is the correspondence between stratospheric flow and synoptic types in the BSR? In particular, what are the frequencies of synoptic types in the BSR from 1979 to 2006 during SSW events? (Evolution in synoptic types during SSWs.)

[13] Our intention through these pair of papers is to provide a more complete description of how the atmosphere affects (and is affected by) stratosphere to troposphere coupling. These processes are key to being able to understand (model) the ocean-sea ice-atmosphere interface and thereby predict the magnitude and direction of change currently evident in the Arctic marine system.

2. Methods

[14] Sudden stratospheric warmings were identified from 1979–2002 following the climatology presented by CP07. According to their vortex detection and classification algorithm, vortex splitting events occurred for the years 1979, 1985, 1987, 1989, and 1999, while vortex displacement

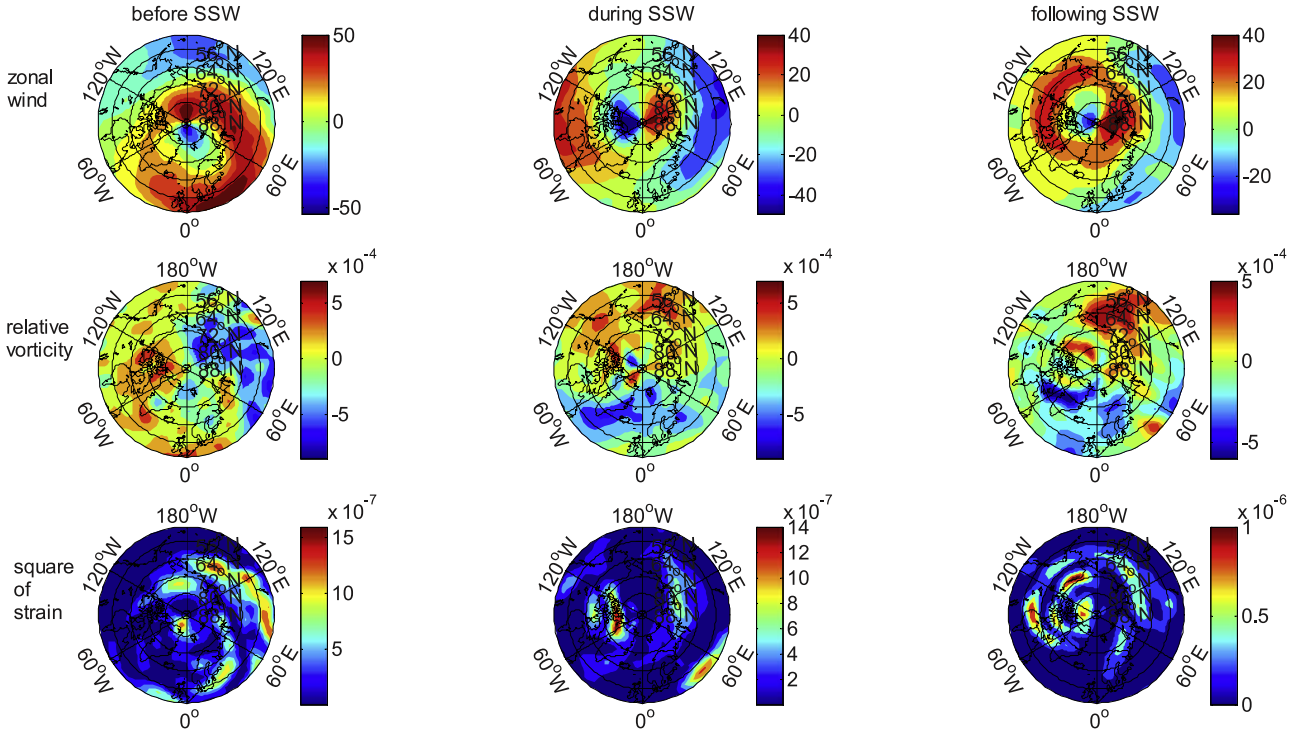

Figure 1a. Stereographic plots of (top) zonal winds, (middle) relative vorticity, and (bottom) square of strain at 10 mbar before (12 March 2000), during (20 March 2000), and following (27 March 2000) sudden stratospheric warmings (SSWs) associated with vortex displacement events.

events occurred for 1980, 1981, 1984, 1987, 1988, 1998, 2000, 2001, and 2002. The year 1987 is distinguished by two SSW events. Additional information on the SSW climatology may be found in Table 1 of CP07. From 2002–2007, SSWs were determined using the same criterion as in CP07, namely by identifying the first day at which a reversal in zonal winds was observed at 10 mbar and at 60°N from November to March of the following year (NDJFM), with final warmings (ten consecutive days prior to April) excluded. SSWs for the analysis extended to 2006 include the years 1979, 1980, 1981, 1984, 1985, 1987, 1988, 1989, 1998, 1999, 2000, 2001, 2004, and 2006. In the absence of the algorithm used to detect vortex displacement and splitting events, wind gradient and synoptic type analyses were conducted for the time interval 1979–2002 for vortex displacement and splitting phenomena.

[15] Daily values of zonal (u) and meridional (v) wind fields were obtained from the NCEP-NCAR reanalysis data at 10 mbar, 100 mbar, 250 mbar, 500 mbar, and 1000 mbar [*Kalnay et al.*, 1996]. Wind gradient fields, namely relative vorticity and square of strain fields, were computed using a first-order finite-differencing scheme. Relative vorticity, defined as $\omega = \partial_x v - \partial_y u$, where x (y) refers to longitudinal (latitudinal) coordinates, and u (v) denote zonal (meridional) wind components, characterizes the rotational component to the flow, and is used to assess cyclonic/anticyclonic activity associated with synoptic-scale activity (and features such as the Beaufort and Aleutian High). By contrast, the square of strain $S^2 = S_n^2 + S_h^2$, for $S_n = \partial_x u - \partial_y v$ the stretching rate, and $S_h = \partial_x v + \partial_y u$, the shear component of the strain, characterizes the nature of stirring, and is used to monitor large-scale straining mechanisms associated with the polar vortex. Gradient wind fields analyzed in the BSR are spatially averaged from 125°W to 165°W longitude.

[16] In order to evaluate the correspondence between gradient wind fields and reversals in mean zonal winds at 60°N, correlation coefficients are computed for winter (NDJFM) from 1979–2007. The evolution in relative vorticity and square of strain is determined by examining composites of the spatially averaged gradient wind fields from 50°N–70°N from 50 days prior to 60 days following the vortex displacement, vortex splitting events, and SSW (vortex displacement and vortex splitting events combined).

[17] We quantify the connections between SSWs and surface cyclonic activity through investigation of the evolution in synoptic types during SSW events. A catalog of 12 daily synoptic weather types in the BSR is presented by Asplin et al. (submitted manuscript, 2008), and the SLP composites shown in Figure 3 therein. Here it was shown that types 1, 6, and 7 are associated with cyclones, and all other types with anticyclones. A well-defined Beaufort High is represented by types 2 and 5. Furthermore, types 1, 3, 4, and 8 were shown to occur during summer months; types 2, 5, 9, 10, 11, and 12 during winter months; type 6 during fall, and 7 throughout the annual cycle (Asplin et al., submitted manuscript, 2008). Distributions of synoptic types are determined in this study for the 1979–2006 time interval during winter (DJFM), as defined in CP07. A predominance and evolution in synoptic types prior to (−50 to −5 days), during (−5 to 20 days), and following (20 to 60 days) the SSW event (day 0) is determined by computing the relative frequency in the number of synoptic types.

[18] In order to investigate possible connections between SSWs and ice motion in the BSR, sea ice relative vorticity is

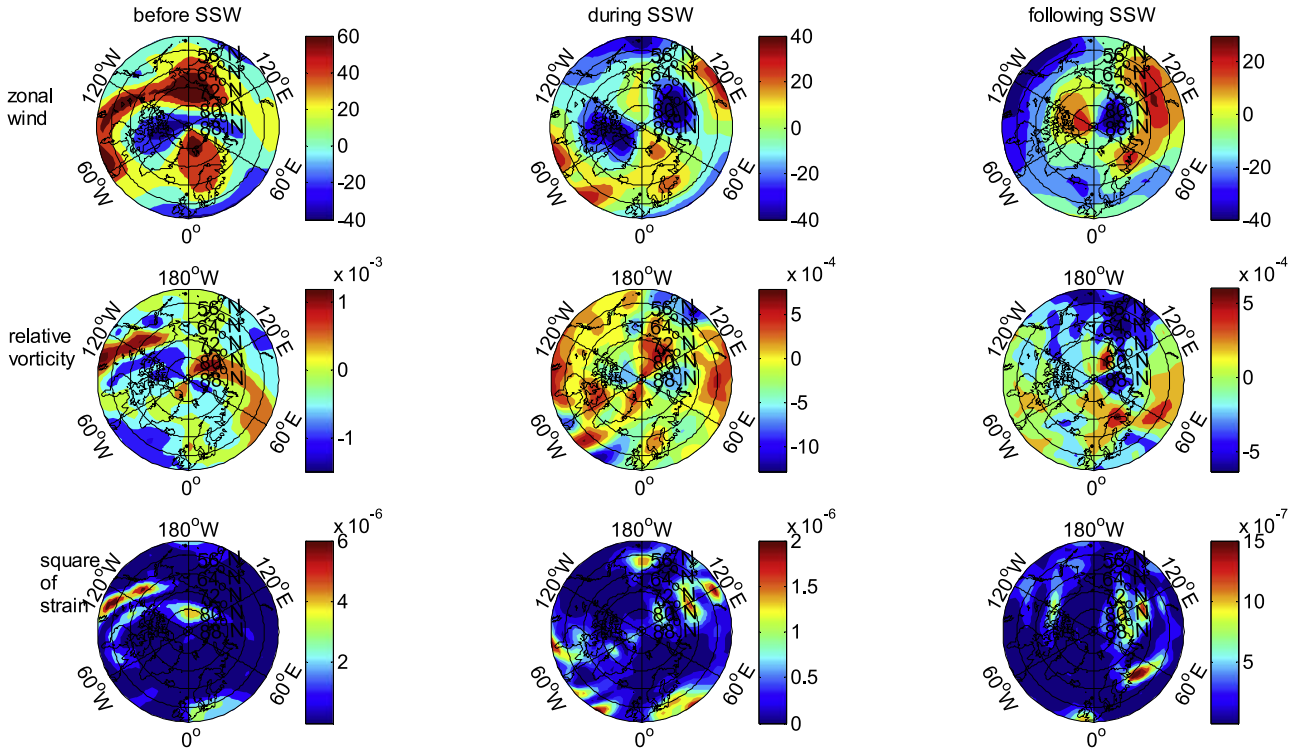

Figure 1b. Stereographic plots from 50°N–90°N of (top) zonal winds, (middle) relative vorticity, and (bottom) square of strain at 10 mbar before (12 February 1989), during (20 February 1989), and following (27 February 1989) SSWs associated with a vortex split event.

used as a measure of sea ice motion and is computed for vortex displacement and splitting events on weekly timescales, from −40 weeks to 40 weeks following SSW events. Sea ice relative vorticity is calculated using weekly sea ice motion vectors from the NSIDC data set transformed to a 361 × 361 EASE grid projection with 25 km spacing, as outlined by *Lukovich and Barber* [2006] and Asplin et al. (submitted manuscript, 2008). In addition, weekly sea ice values obtained from the NSIDC data set were computed from daily AVHRR, SMMR, SSM/I and IABP buoy data following *Fowler* [2003]. Relative vorticity is averaged over the BSR and is used to provide a consistent signature of magnitude and orientation of circulation for the sea ice and atmosphere (a year-week plot of relative vorticity is shown in Figure 6 of Asplin et al. (submitted manuscript, 2008). Differences are computed to highlight timescales over which distinct differences in sea ice phenomena are observed.

3. Results

3.1. SSWs and Stratospheric Wind Gradients

[19] As signatures of perturbations to the polar vortex and reversals in stratospheric zonal winds at 10 mbar and 60°N, SSWs also capture significant erosion in straining mechanisms associated with the polar vortex. Stereographic plots of stratospheric zonal winds, relative vorticity and strain fields before, during and following SSWs illustrate differences between stratospheric gradient wind fields for vortex displacement and split events on 20 March 2000, and 27 February 1989, respectively (Figures 1a and 1b). Displacement in the polar vortex is reflected in the aforementioned comma shape of the strain field (Figure 1a, square of strain following SSW) associated with filamentation. During vortex splitting events, the polar vortex is separated into two vortices, and significant erosion in the square of strain fields is observed (Figure 1b, square of strain following SSW). Remnants of high strain are evident at the periphery of the vortices established following the SSW splitting event. Significant spatial variability is observed in the relative vorticity fields, associated with synoptic activity and small-scale features of the flow. Temporal variability in stratospheric wind gradient fields is reflected in correlation coefficients computed between zonal mean zonal winds and spatially averaged stratospheric relative vorticity and strain fields for different latitude bands during winter (NDJFM) from 1979–2007 (Figure 2). Significant correlations are observed between the square of strain fields spatially averaged from 50°N–90°N and zonal mean winds. Weaker correlations are observed for strain fields computed at 60°N because of spatial variability the position of the polar vortex. Weak correlations between relative vorticity fields spatially averaged from 50°N–90°N are to be expected because of spatial and temporal variability in cyclone/anticyclone activity.

[20] Composites of stratospheric wind gradient fields for all SSW events (Figure 3a) and for vortex displacement and splitting events (Figure 3b) highlight suppression in wind gradients with SSWs and a deceleration in the zonal jet. The evolution in relative vorticity spatially averaged at 60°N, 50°N–70°N, and 50°N–90°N for all SSW events (years associated with vortex splitting and displacement events combined) demonstrates a rapid descent in gradient fields at

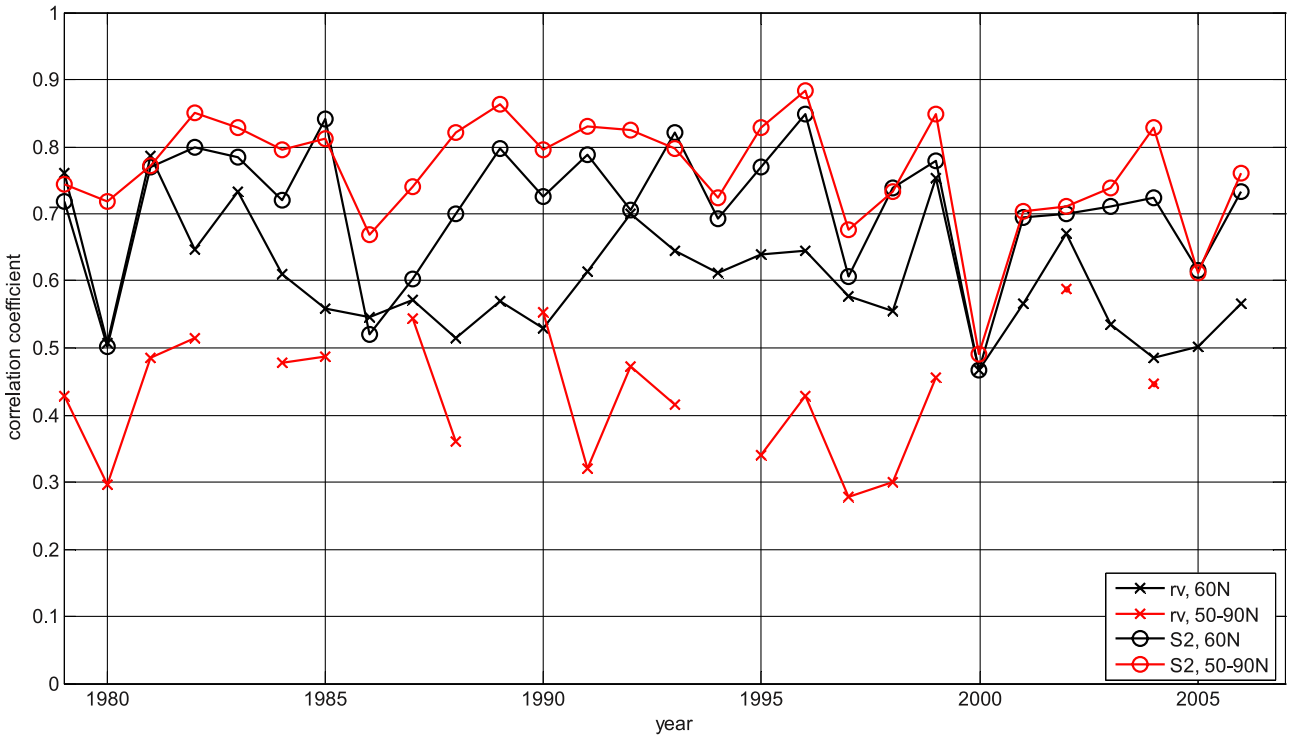

Figure 2. Running correlation coefficients from 1979–2007 between zonal mean zonal winds and relative vorticity and strain fields at 60°N (black lines) and 50°N–90°N (red lines) during SSW winter (NDJFM).

the time of the SSW, particularly for the 50°N–70°N latitude band (Figure 3a, left). Lower relative vorticity values for spatially averaged relative vorticity poleward of 50°N reflect spatial averaging over a combination of cyclones and anticyclones. Fluctuations in relative vorticity are observed following the SSW, which we speculate to be an artifact of the formation of cyclonic and anticyclonic filaments associated with erosion of the polar vortex. The

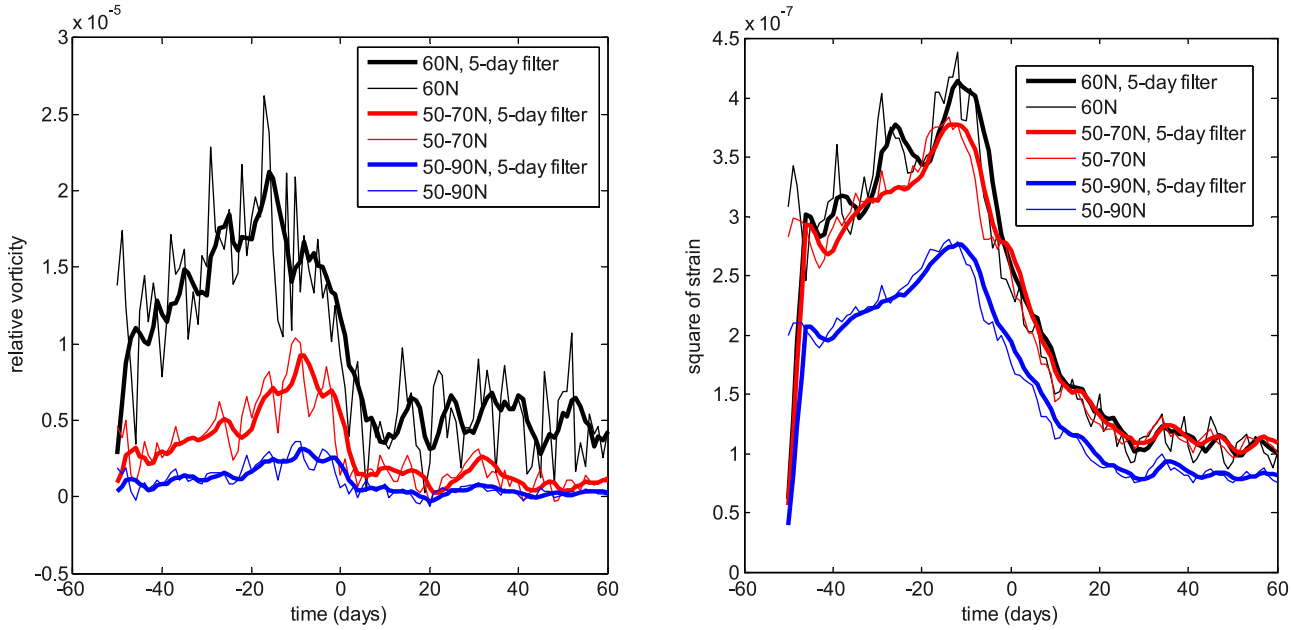

Figure 3a. Evolution in (left) spatially averaged relative vorticity and (right) square of strain at 10 mbar 60°N (black line), 50°N–70°N (red line), and 50°N–90°N (blue line) latitude bands for all (split and displacement) SSW events. Day 0 corresponds to the reversal in winds associated with the SSW. Solid lines indicate 5-day filtered data.

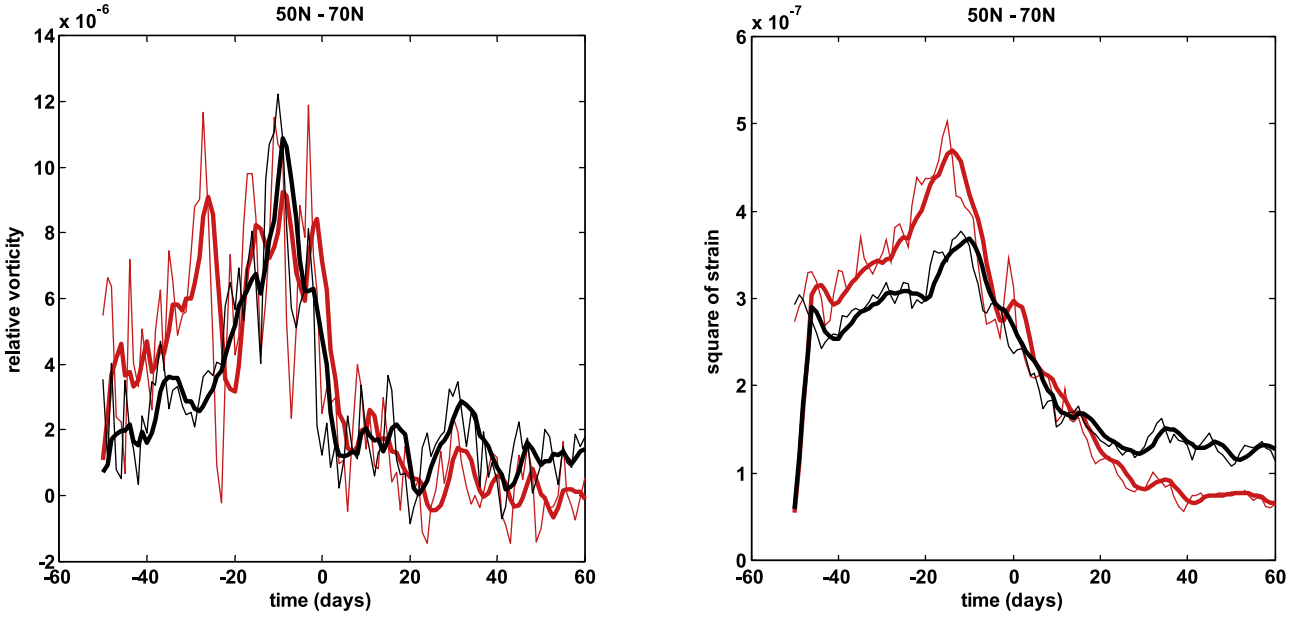

Figure 3b. Evolution in (left) relative vorticity and (right) square of strain at 10 mbar, averaged from 50°N–70°N, during vortex split (red lines) and displacement (black lines) SSW events. Day 0 corresponds to the SSW event. Solid lines indicate 5-day filtered relative vorticity and square of strain values.

strain field exhibits significantly less variability than the relative vorticity fields, with decay in strain that equilibrates after approximately 20 days (Figure 3a, right).

[21] It should also be noted that relative vorticity computed from 50°N to 70°N encompasses the 60°N latitude band associated with SSWs, while also capturing cyclonic activity at the periphery of the polar vortex as well as possible poleward displacements in cyclonic activity resulting from displacements in the zonal jet: when examined from 50 to 90°N relative vorticity diagnostics also capture the circulation associated with the polar vortex.

[22] The evolution in stratospheric relative vorticity fields from 50°N–70°N during vortex split and displacement events (Figure 3b, left) exhibits distinctive behavior prior to and following the SSW event. For vortex splitting, a peak in cyclonic activity occurs 30 days prior to the SSW, with a second peak immediately preceding the SSW event. We speculate that an interruption in cyclonic activity may be

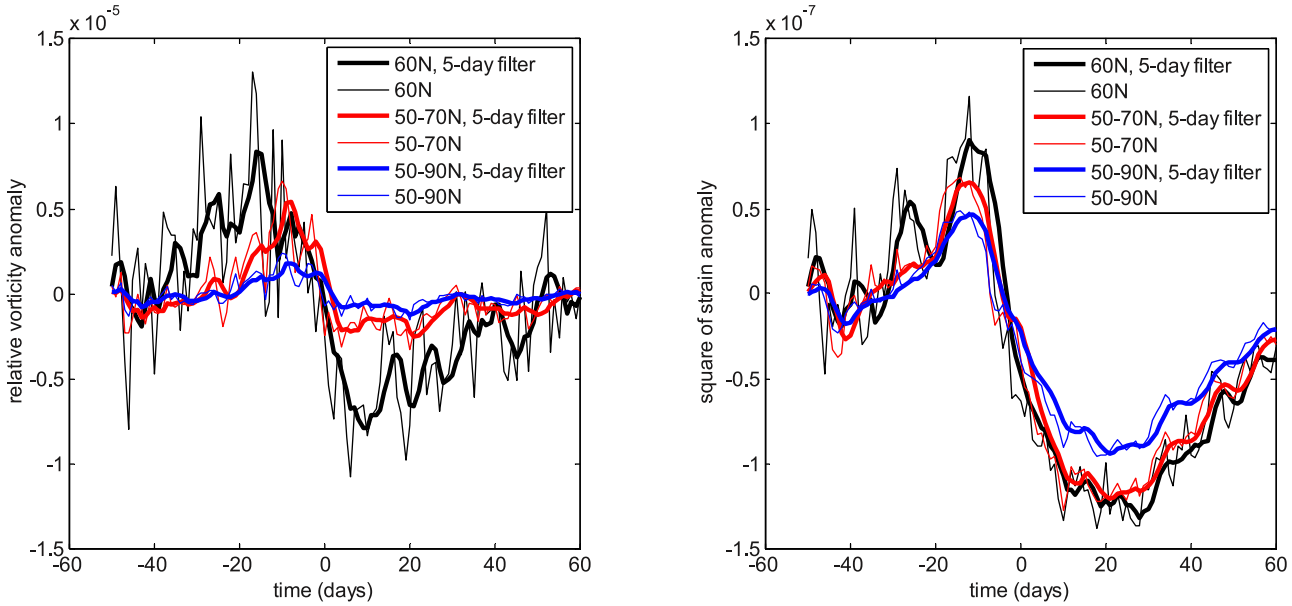

Figure 4a. Evolution in (left) spatially averaged relative vorticity anomalies and (right) square of strain anomalies, at 60°N (black line), 50°N–70°N (red line), and 50°N–90°N (blue line) latitude bands for all (split and displacement) SSW events.

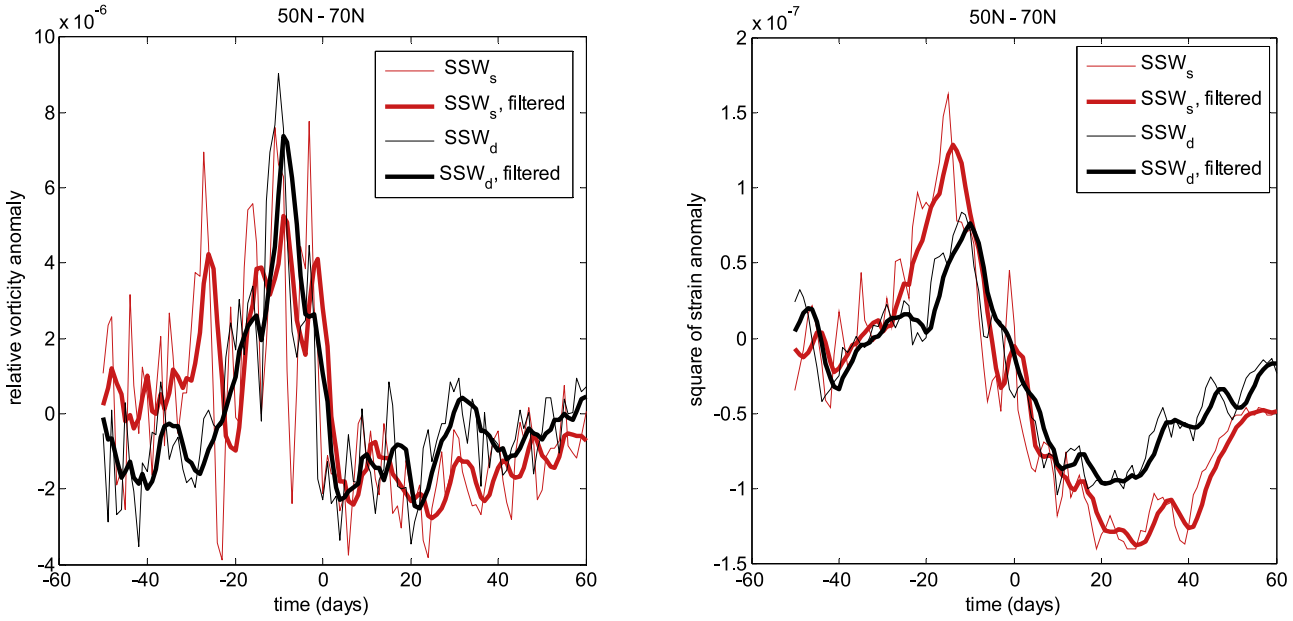

Figure 4b. Evolution in (left) relative vorticity anomalies and (right) square of strain anomalies at 10 mbar, averaged from 50°N–70°N, during vortex split (red lines) and displacement (black lines) SSW events.

attributed to the aforementioned merging of anticyclones during vortex displacements studied by *Harvey et al.* [2002]. Following the SSW for vortex splitting, relative vorticity continues to decline and exhibits anticyclonic activity, which is consistent with an increase in anticyclonic activity at the expense of a significant disruption in the polar vortex documented by *Harvey et al.* [2002]. By contrast, for vortex displacements, cyclonic activity begins to increase 20 days prior to the SSW event, and fluctuates between positive and negative values following the SSW displacement event.

[23] The evolution in strain fields from 50°N to 70°N during vortex split and displacement events (Figure 3b, right), further highlights differences in strain fields before and after distinctive SSW events. In particular, a much more rapid descent is observed in the strain fields for vortex splitting relative to vortex displacement events (note the difference in peak heights approximately 20 to 15 days prior to SSW events). The square of strain equilibrates following vortex displacements, and continues to decline following vortex splits, as is also evidenced in Figure 1b, square of strain following SSW.

[24] Also of interest in establishing connections between SSWs and gradient wind fields are their anomalies, or departures from the 1979–2006 climatological mean (Figures 4a and 4b). Noteworthy are differences in the evolution of relative vorticity anomalies preceding SSWs, in contrast to strain anomalies, for all SSW events (Figure 4a). Negative vorticity anomalies exist approximately 20 days prior to the SSW event (Figure 4b, left). Both positive and negative relative vorticity anomalies exist following vortex displacements, which may be a signature of cyclone/anticyclone development during filamentation, while negative anomalies persist following vortex splitting events. Negative strain anomalies exist following vortex displacements, demonstrating degradation of the straining mechanisms associated with the polar vortex (Figure 4b, right).

[25] In the paper by Asplin et al. (submitted manuscript, 2008), a catalogue of synoptic types was established that identified surface synoptic weather types in the BSR. Since one of our primary objectives in this study is to explore the connection between reversals in stratospheric winds and surface synoptic types, we examine the manifestation of SSWs in the BSR through analysis of the evolution in wind gradients averaged over the BSR (Figure 5), and quantify this connection based on the synoptic type catalogue developed by Asplin et al. (submitted manuscript, 2008). Noteworthy in the evolution of relative vorticity fields is the presence of anticyclonic activity during, and for approximately 20 days following, all SSWs (Figure 5a), suggesting a predominance of anticyclones in the BSR. Anticyclonic activity is observed approximately 35 days before vortex splitting events in the BSR (Figure 5c), while cyclonic activity precedes vortex displacement events. Anticyclonic activity characterizes relative vorticity during the SSW event, while cyclonic activity exists approximately 20 (40) days following vortex (displacement) splitting events. Also of interest is the sharp decline in strain beginning approximately 10 days prior to all (vortex displacement and splits combined) SSWs and continuing following all SSWs (Figure 5b). A sharp descent is also observed in strain fields prior to SSW splitting events, with a continued decline following SSWs depicting erosion in strain associated with the polar vortex (Figure 5d).

3.2. Stratosphere-Surface Evolution in Wind Gradients During SSW Events

[26] The evolution in wind gradient fields from the stratosphere to the surface demonstrates significant variability in surface relative vorticity compared to surface strain fields (Figure 6). Cyclonic activity exists near the surface in localized regions for 30 to 40 days prior to all SSW events,

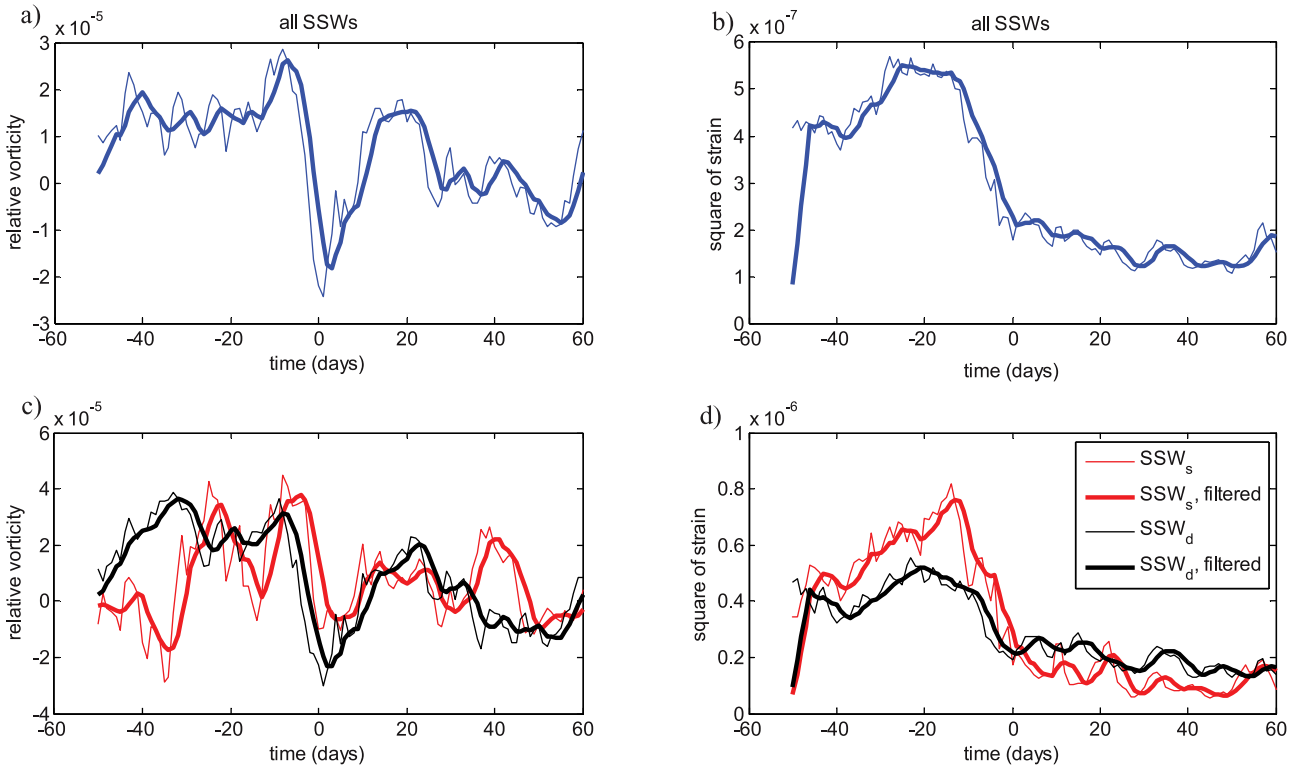

Figure 5. Evolution in (a, c) relative vorticity and (b, d) square of strain at 10 mbar, spatially averaged over the BSR (125°W–165°W), for all SSWs (Figures 5a and 5b), and during vortex split (red lines) and displacement (black lines) SSW events.

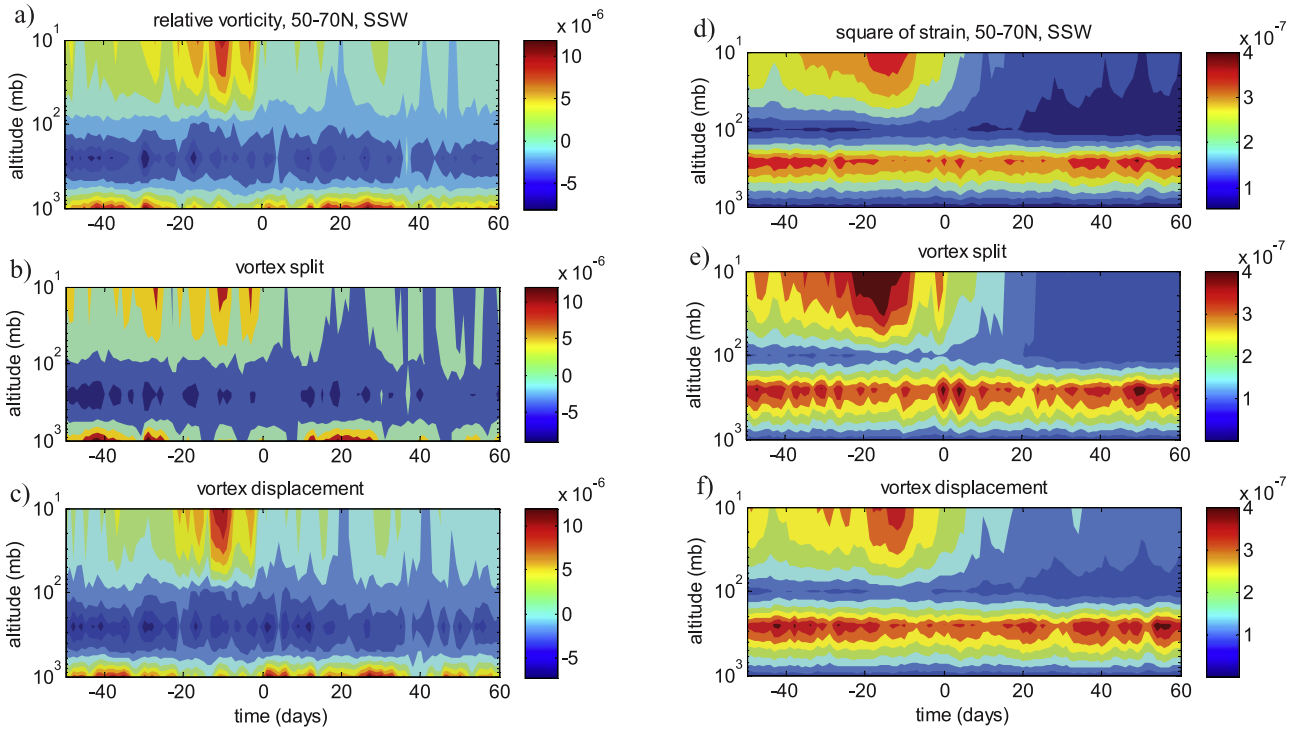

Figure 6. Time-height diagram of (a, b, c) relative vorticity and (d, e, f) square of strain, spatially averaged from 50°N–70°N for all SSWs (Figures 6a and 6d), and during vortex split (Figures 6b and 6e) and displacement (Figures 6c and 6f) SSW events.

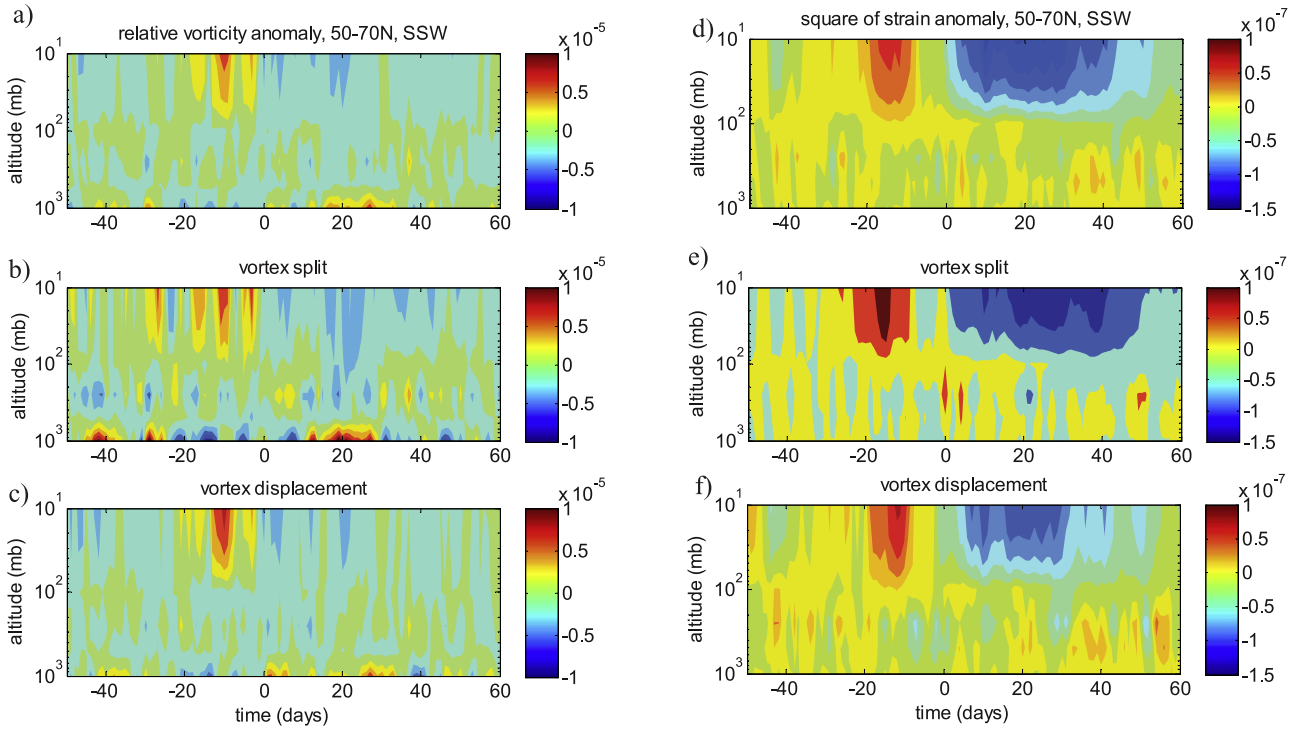

Figure 7. Time-height diagram of evolution in (a, b, c) relative vorticity anomalies and (d, e, f) square of strain anomalies, spatially averaged from 50°N–70°N, for all SSWs (Figures 7a and 7d), and during vortex split (Figures 7b and 7e) and displacement (Figures 7c and 7f) SSW events.

and from approximately days 15 to 35 following vortex events (Figure 6a). During vortex splitting events, cyclonic activity is localized in bands centered at 40 and 10 days prior to the SSW event and 10 days following the SSW event, while stratospheric relative vorticity exhibits episodic intervals of cyclonic activity beginning approximately 30 days prior to the SSW that cease following the SSW. During vortex displacement events, cyclonic activity exhibits a maximum (minimum) in the stratosphere (surface) during the interval 10 days prior to the SSW. The absence of features near the surface during SSWs for the strain fields illustrates the dominance of straining mechanisms in the polar stratosphere (Figures 6d, 6e, and 6f).

[27] The manifestation of SSWs in wind gradient fields at hemispheric scales is further illustrated in the evolution of relative vorticity and strain anomalies from the stratosphere to the surface (Figure 7). Demonstrated in particular is the interval of positive relative vorticity anomalies approximately 10 to 20 days prior to all SSWs, as discussed in the previous section, followed by positive anomalies near the surface from approximately 17 to 30 days following all SSWs events (Figure 7a). During vortex splitting events, alternating positive and negative relative vorticity anomalies are observed near the tropopause prior to and following vortex splits. Negative relative vorticity anomalies are observed near the surface prior to vortex splits, while positive anomalies are established approximately 15 days following vortex splits and less coherent positive anomalies are observed approximately 30 days following vortex displacements (Figures 7a, 7b, and 7c). Strain anomalies emphasize an extended duration (~50 days) in reduced strain following vortex splits, in comparison with the duration of negative strain anomalies (~30 days) following vortex displacements (Figures 7d, 7e, and 7f).

[28] Examination of the evolution in relative vorticity and strain fields and their anomalies averaged over the BSR underlines the connection between stratospheric and regional surface phenomena (Figures 8 and 9). Noteworthy is the band of anticyclonic activity that extends from the stratosphere to the surface during vortex splitting events (depicted by the blue band near t = 0), which acts as a "window" from the surface to the stratosphere (Figure 8b). This feature resembles the aforementioned well of anticyclonic activity from 65°N–85°N associated with the Aleutian High and displacement of the polar vortex toward the dateline [*Harvey et al.*, 2002]. The authors speculate that anticyclonic activity during SSWs may be a signature of advection of the Aleutian High into the BSR during SSWs, or a signature of strengthening in the Beaufort High. The band of anticyclonic activity extends only to the tropopause (250 mbar) during (near t = 0), in a manner consistent with the aforementioned 2–6 day synoptic timescale associated with baroclinic waves found in response to changes in Arctic ice cover [*Sokolova et al.*, 2007], and at 30 days after the SSW event for all SSWs and for vortex displacement SSWs (Figures 8a and 8c). In addition, relative vorticity is characterized by predominantly cyclonic activity from the surface to the tropopause following vortex splitting events in the BSR, which lasts for approximately 30 days. Strain fields in the BSR exhibit behavior comparable to hemispheric scale strain fields (compare Figures 6a, 6b, and 6c with Figures 8a, 8b, and 8c).

[29] The window of anticyclonic activity that extends from the stratosphere to the surface during SSW events in

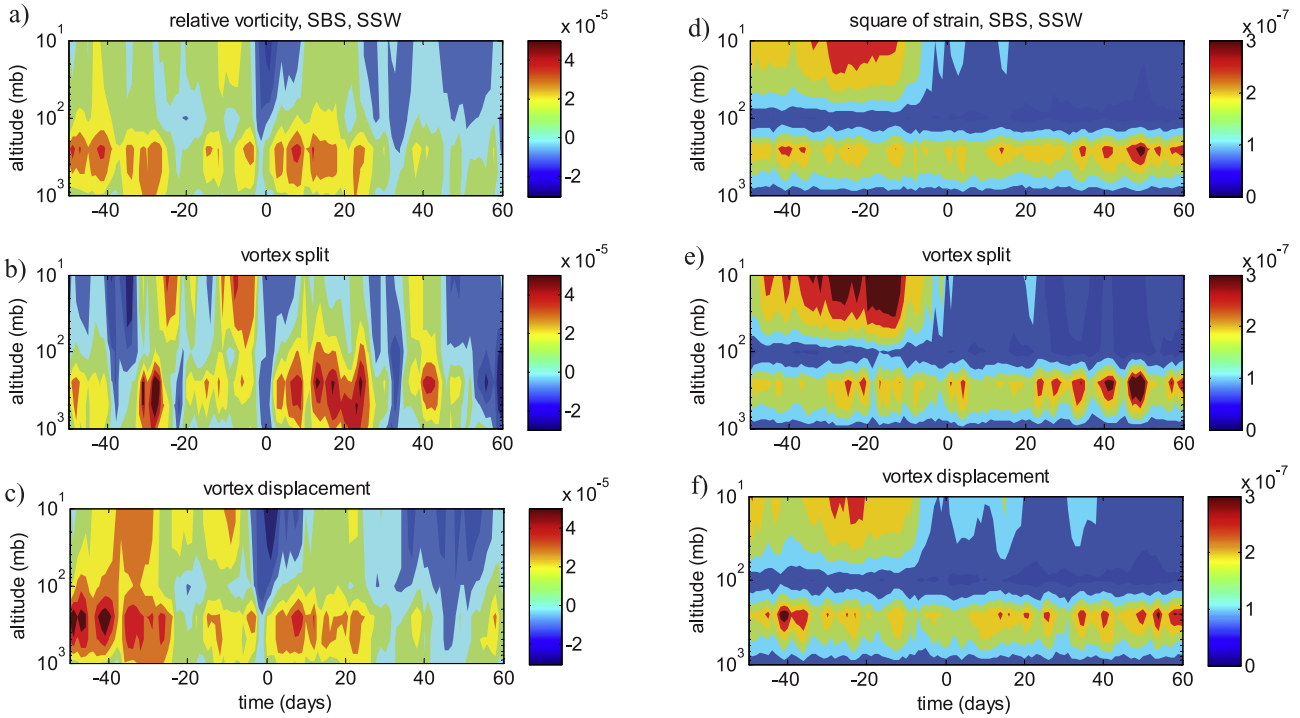

Figure 8. Time-height diagram of evolution in (a, b, c) relative vorticity and (d, e, f) square of strain, spatially averaged over the Beaufort Sea region for all SSWs (Figures 8a and 8d), and during vortex split (Figures 8b and 8e) and displacement (Figures 8c and 8e) SSW events.

the BSR is evident also in the time-height evolution in relative vorticity anomalies in the BSR (blue band, Figures 9a, 9b, and 9c). In particular, a band of negative anomalies exists between the stratosphere and surface near t = 0, for both vortex splitting and displacement events (Figures 9b and 9c). However, as previously discussed,

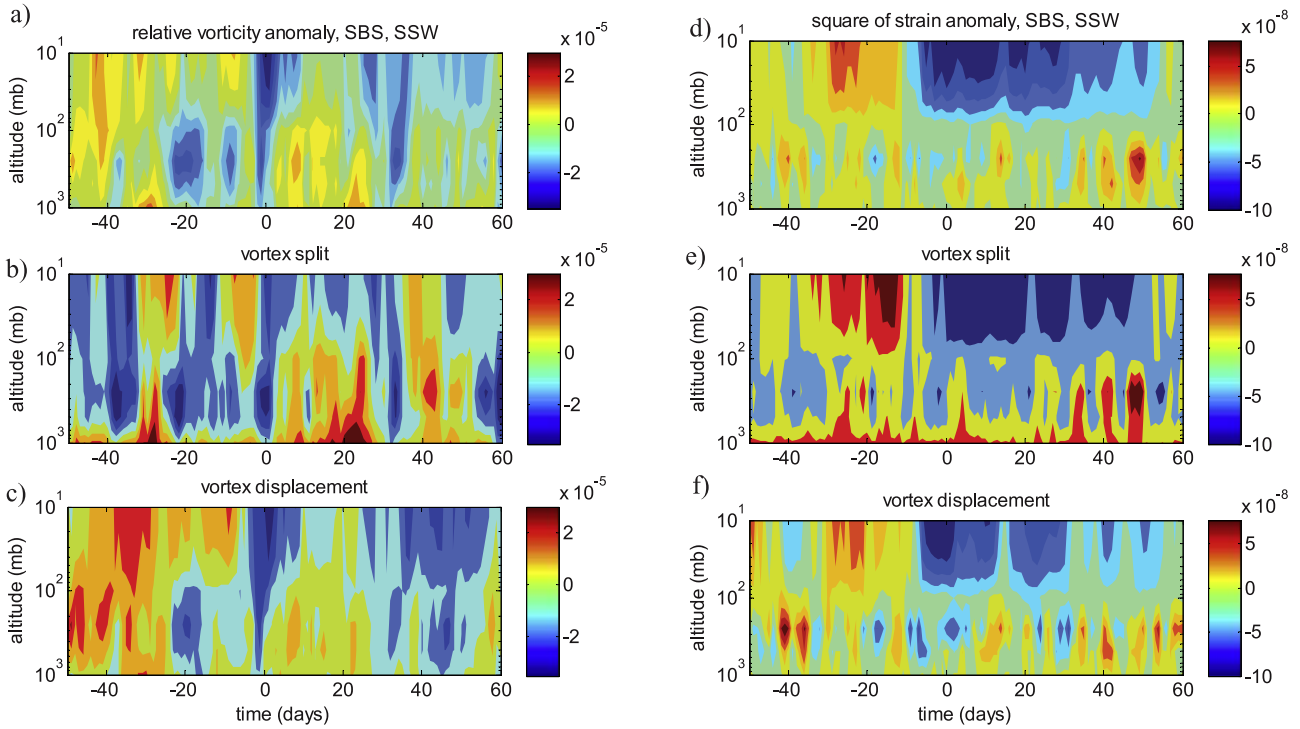

Figure 9. Time-height diagram of evolution in (a, b, c) relative vorticity anomalies and (d, e, f) square of strain anomalies, spatially averaged over the Beaufort Sea region for all SSWs (Figures 9a and 9d), and during vortex split (Figures 9b and 9e) and displacement (Figures 9c and 9f) SSW events.

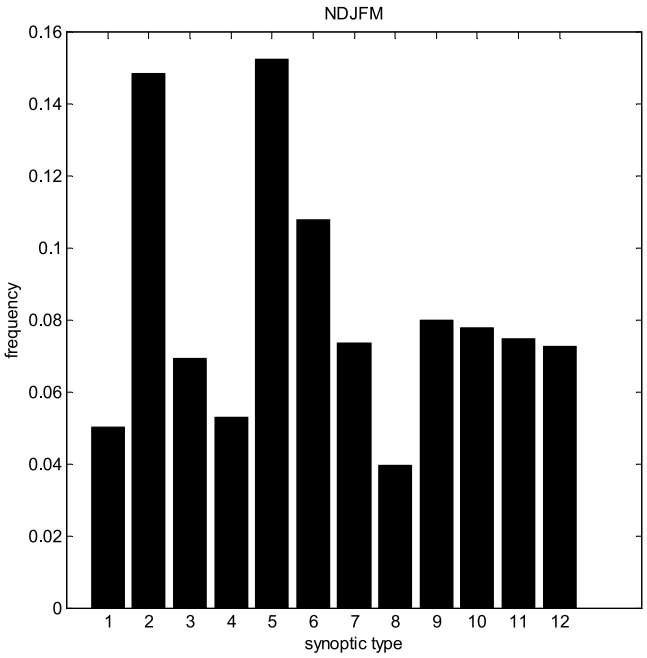

Figure 10. Relative frequency of synoptic types during winter (NDJFM) from 1979–2006.

negative relative vorticity during vortex displacement events exists only from the stratosphere to the tropopause: vanishing cyclonic activity exists from the surface to the troposphere (Figure 8c). The presence of negative anomalies in Figure 9 suggests an advection of anticyclones into the BSR that cancels cyclonic activity during SSWs. Also of interest are positive relative vorticity anomalies in the BSR near the surface 20 days after vortex splitting events that extend to the lower stratosphere (red band near t = 20 in Figure 9b). Noteworthy features in the strain anomaly fields include the presence of positive anomalies near the tropopause following vortex splitting events (Figure 9e).

3.3. Evolution in Synoptic Types During SSWs

[30] Distributions of synoptic types Asplin et al. (submitted manuscript, 2008) during winter (NDJFM) for all years from 1979–2007 exhibit high frequencies in cyclone types 2, 5, and 6, in a manner consistent with the seasonal distribution of synoptic types outlined by Asplin et al. (submitted manuscript, 2008) (Figure 10). As noted previously, types 2 and 5 characterize the Beaufort High centered over the BSR and anticyclonic circulation, while type 6 depicts a low located to the west of Ellesmere Island, which corresponds to cyclonic circulation in the BSR.

[31] Distributions of synoptic types for vortex split and displacement events during winter indicate that type 5 predominates during vortex displacements, while types 2, 5 and 9 predominate during vortex splits, all of which depict anticyclonic activity (Figure 11). Analysis of a χ^2 two-sample test [*Wall and Jenkins*, 2003] to determine whether the occurrence of synoptic types varies for vortex splitting and displacement events results in a rejection of the null hypothesis of their statistical independence ($\chi^2 \sim 30.4 >$ 24.7 for 11 degrees of freedom and significance level 0.01). In particular, types 2 and 5 capture a strengthened Beaufort High over the BSR, while type 9 characterizes a high located in the western segment of the BSR (Asplin et al., submitted manuscript, 2008, Figure 3). Synoptic types 10 and 11, representing the Aleutian Low and its eastward displacement, also occur during vortex displacement events, albeit less often. These results, namely predominance in synoptic types 2 and 5 for both vortex displacements and splits suggest that SSWs are manifested at the regional scale by a strengthened Beaufort High associated with types 2 and 5. It is interesting to note that type 5 includes a cyclonic component associated with the Aleutian Low; the coexistence of a cyclone and anticyclone for this synoptic type may account for vanishing relative vorticity evident during SSW displacements, and shown in Figure 8c. By contrast, type 2 is governed by the Beaufort High, providing further evidence for the window of anticyclonic activity observed in the evolution of relative vorticity gradients from the surface to the stratosphere during SSWs shown in Figure 8b.

[32] Of particular interest is the evolution in frequency of synoptic types during SSW events (Figure 12). Noteworthy are high frequencies in synoptic types 2 and 5 characteristic of a strengthened Beaufort High during SSWs (Figures 12b and 12e). Investigation of frequencies in synoptic types leading up to SSWs exhibits high frequencies in synoptic type 5 for all SSW years (Figure 12a). In addition, winter anticyclone types 5 and 2 (11) occur most often for vortex splits (displacements) (Figure 12d). During SSWs a doubling in frequencies of wintertime anticyclones is observed; type 2 (5) dominates during SSW split (displacement) events, so that the BSR during all SSW events is characterized by a strengthened Beaufort High (Figures 12b and 12e). Differences in frequencies for synoptic types associated with wintertime anticyclones during vortex displacement and split events may be a result of the time interval considered: as shown in Figure 8, cyclonic activity persists near the surface for 20 days following vortex splits

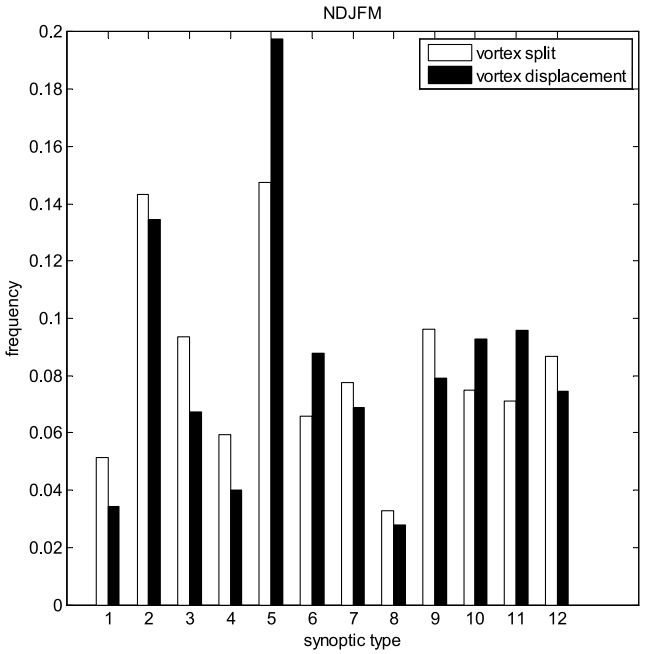

Figure 11. Relative frequency of synoptic types for SSW years characterized by vortex split (white bar) and displacement (black bar) events.

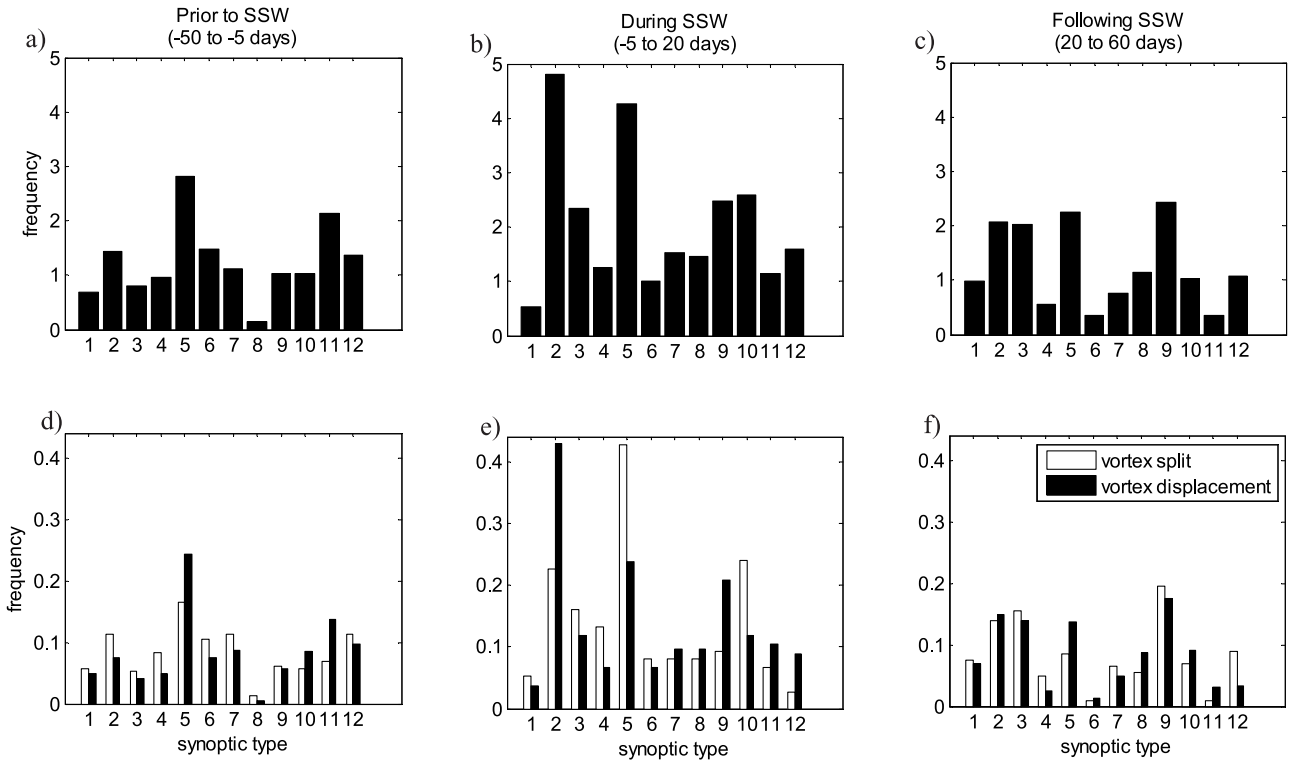

Figure 12. Distribution of frequencies in synoptic types (a, d) before (−50 to −5 days), (b, e) during (−5 to 20 days), and (c, f) following (20 to 60 days) SSWs, for all SSW events (Figures 12a, 12b, and 12c), and for vortex split and displacement events (Figures 12d, 12e, and 12f).

(Figure 8b), while weaker cyclonic activity is observed during this same time frame following vortex displacements (Figure 8c). Following SSWs, a collapse in synoptic types associated with anticyclones is observed, and the state of the BSR following both displacement and splitting events is captured by slightly higher frequencies in type 9, characteristic of a weakened Beaufort High (Figures 12c and 12f). These results demonstrate an increase in the number of anticyclones and concomitant strengthening (weakening) of the Beaufort High during (following) SSWs, providing a signature of the correspondence between stratospheric flow and surface cyclone types in the BSR.

3.4. SSWs and Sea Ice Motion

[33] Our motivation for using wind gradient fields as a diagnostic in examining stratosphere-surface coupling in the BSR is to capture both large- and small-scale features of the flow, and to provide a consistent measure of circulation for atmospheric and sea ice phenomena. In this section we examine sea ice motion in the context of vortex splitting and

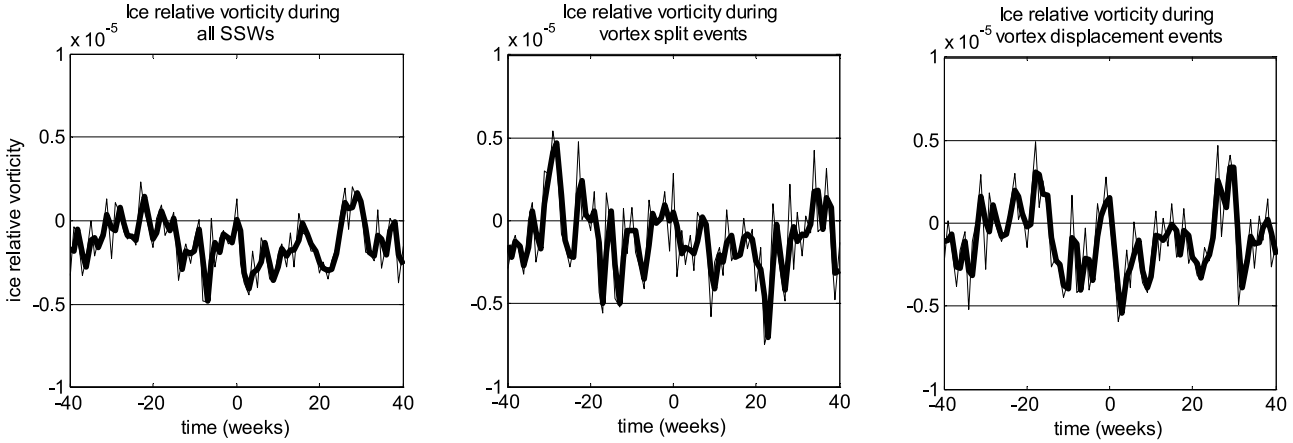

Figure 13. Evolution in ice relative vorticity in the Beaufort Sea Region for (left) all SSWs, (middle) stratospheric vortex splitting events, and (right) stratospheric displacement events as a function of week from 1979–2006. Solid lines indicate two-week filtered data.

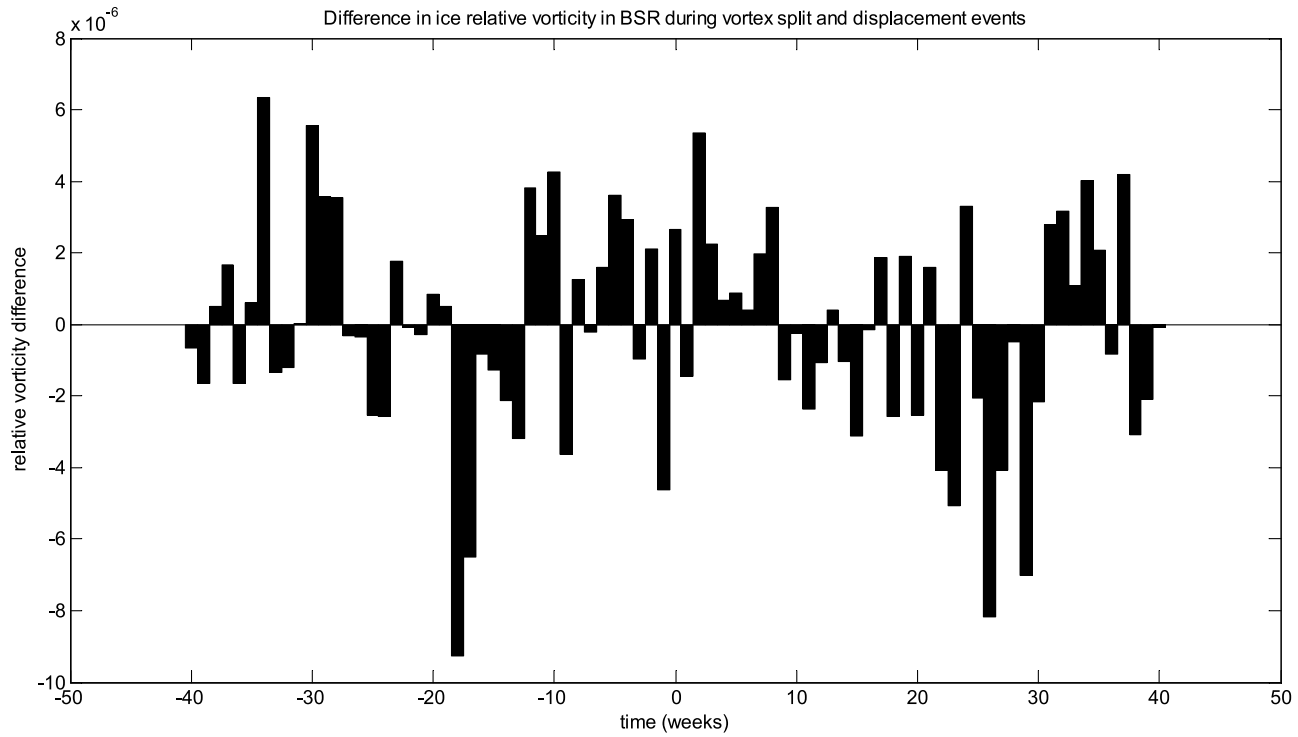

Figure 14. Difference between ice relative vorticity in BSR for stratospheric vortex splitting event and ice relative vorticity in BSR for stratospheric vortex displacement event.

displacement events, using relative vorticity as a measure for sea ice motion. Investigation of weekly sea ice relative vorticity in the BSR during vortex displacement and splitting events shows weaker anticyclonic circulation for stratospheric vortex split events than for vortex displacement events for about seven weeks following SSWs (Figures 13 and 14). Significant differences in BG circulation are observed during stratospheric vortex displacement and splitting events on longer timescales, with an out-of-phase relationship evident at ~18 weeks prior to SSWs, with strong anticyclonic (cyclonic) circulation for stratospheric vortex split (displacement) events (Figure 13). Significant differences are also observed near weeks 20 to 30 following SSWs. Noteworthy also is the existence of strong cyclonic circulation in the BG for vortex splitting events that precedes cyclonic circulation for vortex displacements by approximately 12 to 15 weeks leading up to the SSW. By contrast, a continued decline in relative vorticity (increase in anticyclonic activity) is observed following SSW splitting events until week 20. The results from this analysis show that significant differences in BG circulation for stratospheric displacement and splitting events are manifested in timescales on the order of several months, both prior to and following SSW events. It should be emphasized, however, that these results only highlight differences in sea ice relative vorticity between vortex splitting and displacement events, and cannot be attributed solely to atmospheric phenomena. Changes in sea ice for timescales greater than one month may be a consequence of oceanic and/or atmospheric forcing mechanisms, the relative roles of which can be determined from a detailed investigation of both atmospheric and oceanic dynamic contributions (from ocean current data), energy and momentum budgets, and feedback mechanisms therein. The physics controlling these empirical observations remains as a priority for further research.

4. Conclusions

[34] Asplin et al. (submitted manuscript, 2008) presented a catalogue of synoptic types and investigated connections between synoptic sea level pressure types preceding summer BG sea ice reversals. In this paper we explored the connection between stratospheric and surface variability in the BSR in the context of SSWs and synoptic types. The results from this analysis suggest a correspondence between stratospheric dynamic variability and surface synoptic types in the BSR, following the climatology for SSWs in the context of vortex displacement and split events developed by *Charlton and Polvani* [2007a], and the climatology for synoptic types in the BSR developed by Asplin et al. (submitted manuscript, 2008). Investigation of our first research question shows that SSWs suppress stratospheric wind gradients, as is evidenced in a rapid descent in relative vorticity during SSWs and decay in strain that equilibrates after approximately 20 days. Stratospheric wind gradients averaged over the BSR demonstrate anticyclonic activity during SSWs that persists for approximately 20 days, providing a regional signature of hemispheric-scale changes in stratospheric variability.

[35] Examination of the evolution in wind gradient fields and their anomalies from the stratosphere to the surface during SSWs demonstrates a band of anticyclonic activity that extends from the stratosphere to the surface during SSWs. Investigation of the evolution in synoptic types during SSWs demonstrates an increase in the number of anticyclones and concomitant strengthening of the Beaufort

High during SSWs, thereby providing a signature of the correspondence between stratospheric flow and surface cyclone types in the BSR. An interesting avenue for future research includes an extension of this analysis to explore the predictive skill of zonal wind anomalies, horizontal wind gradients, and anticyclone development in the BSR.

References

Baldwin, M. P., and T. J. Dunkerton (2001), Stratospheric harbingers of anomalous weather regimes, *Science*, *294*, 581–584, doi:10.1126/science.1063315.

Baldwin, M. P., D. B. Stephenson, D. W. J. Thompson, T. J. Dunkerton, A. J. Charlton, and A. O'Neill (2003), Stratospheric memory and skill of extended-range forecasts, *Science*, *301*, 636–639, doi:10.1126/science.1087143.

Charlton, A. J., and L. M. Polvani (2007a), A new look at stratospheric sudden warmings. Part I: Climatology and modeling benchmarks, *J. Clim.*, *20*, 449–469, doi:10.1175/JCLI3996.1.

Charlton, A. J., and L. M. Polvani (2007b), A new look at stratospheric sudden warming. Part II: Evaluation of numerical model simulations, *J. Clim.*, *20*, 470–487, doi:10.1175/JCLI3994.1.

Comiso, J. C. (2006), Abrupt decline in the Arctic winter sea ice cover, *Geophys. Res. Lett.*, *33*, L18504, doi:10.1029/2006GL027341.

Deser, C., J. E. Walsh, and M. S. Timlin (2000), Arctic Sea ice variability in the context of recent atmospheric circulation trends, *J. Clim.*, *13*, 617–633, doi:10.1175/1520-0442(2000)013<0617:ASIVIT>2.0.CO;2.

Drobot, S., and J. A. Maslanik (2003), Interannual variability in summer Beaufort Sea ice conditions: Relationship to winter and summer surface and atmospheric variability, *J. Geophys. Res.*, *108*(C7), 3233, doi:10.1029/2002JC001537.

Fowler, C. (2003), Polar pathfinder daily 25 km EASE-grid sea ice motion vectors, http://nsidc.org/data/nsidc-0116.html, Natl. Snow and Ice Data Cent., Boulder, Colo.

Harvey, F., V. Lynn, R. B. Pierce, T. D. Fairlie, and M. Hitchmann (2002), A climatology of stratospheric polar vortices and anticyclones, *J. Geophys. Res.*, *107*(D20), 4442, doi:10.1029/2001JD001471.

Kalnay, E., et al. (1996), The NCEP/NCAR 40-year reanalysis project, *Bull. Am. Meteorol. Soc.*, *77*, 437–471, doi:10.1175/1520-0477(1996)077<0437:TNYRP>2.0.CO;2.

Lukovich, J. V., and D. G. Barber (2006), Atmospheric controls on sea ice motion in the southern Beaufort Sea, *J. Geophys. Res.*, *111*, D18103, doi:10.1029/2005JD006408.

Manney, G. L., K. Kruger, J. Sabutis, S. A. Sena, and S. Pawson (2005), The remarkable 2003–2004 winter and other recent warm winters in the Arctic stratosphere since the late 1990s, *J. Geophys. Res.*, *110*, D04107, doi:10.1029/2004JD005367.

Maslanik, J. A., S. D. Drobot, C. Fowler, W. Emery, and R. Barry (2007), On the Arctic climate paradox and the continuing role of atmospheric circulation in affecting sea ice conditions, *Geophys. Res. Lett.*, *34*, L03711, doi:10.1029/2006GL028269.

Overland, J. E., and M. Wang (2005), The third Arctic climate pattern, *Geophys. Res. Lett.*, *32*, L23808, doi:10.1029/2005GL024254.

Polvani, L. M., and D. Waugh (2004), Upward wave activity flux as a precursor to extreme stratospheric events and subsequent anomalous surface weather regimes, *J. Clim.*, *17*, 3548–3554, doi:10.1175/1520-0442(2004)017<3548:UWAFAA>2.0.CO;2.

Scott, R. K., and L. M. Polvani (2006), Internal variability of the winter stratosphere. Part I: Time-independent forcing, *J. Atmos. Sci.*, *63*, 2758–2776, doi:10.1175/JAS3797.1.

Shepherd, T. G. (2002), Issues in stratosphere-troposphere coupling, *J. Meteorol. Soc. Jpn.*, *80*(4B), 769–792, doi:10.2151/jmsj.80.769.

Sokolova, E., K. Dethloff, A. Rinke, and A. Benkel (2007), Planetary and synoptic scale adjustment of the Arctic atmosphere to sea ice cover changes, *Geophys. Res. Lett.*, *34*, L17816, doi:10.1029/2007GL030218.

Strahan, S. (2002), Influence of planetary wave transport on Arctic ozone as observed by Polar Ozone and Aerosol Measurement (POAM) III, *J. Geophys. Res.*, *107*(D20), 4417, doi:10.1029/2002JD002189.

Thompson, D. W. J., M. P. Baldwin, and J. M. Wallace (2002), Stratospheric connection to Northern Hemisphere wintertime weather: Implications for prediction, *J. Clim.*, *15*, 1421–1428, doi:10.1175/1520-0442(2002)015<1421:SCTNHW>2.0.CO;2.

Wall, J. V., and C. R. Jenkins (2003), *Practical Statistics for Astronomers*, 277 pp., Cambridge Univ. Press, New York.

M. G. Asplin, D. G. Barber, and J. V. Lukovich, Centre for Earth Observation Science, Faculty of Environment, Earth, and Resources, University of Manitoba, Winnipeg, MB R3T 2N2, Canada. (lukovich@cc.umanitoba.ca)